Journal of Peptide Science
J. Peptide Sci. **5**: 313–322 (1999)

Assembly of Binding Loops on Aromatic Templates as VCAM-1 Mimetics

FRANCESCO PERI[a], DANIEL GRELL[a], PASCAL DUMY[a], YOSHIHIRO YOKOKAWA[a], KARL WELZENBACH[b], GABRIELE WEITZ-SCHMIDT[b] and MANFRED MUTTER[a,*]

[a] Institute of Organic Chemistry, University of Lausanne, BCH-Dorigny, Lausanne, Switzerland
[b] Novartis Pharma AG, Transplantation Research, Basel, Switzerland

Received 4 January 1999
Accepted 20 January 1999

Abstract: The design and synthesis of cyclic mimetics of VCAM-1 protein that reproduce the integrin-binding domain are presented. The unprotected peptide precursor **37–43**, Thr-Gln-Ile-Asp-Ser-Pro-Leu, was grafted onto functional templates of type naphthalene, biphenyl and benzyl through the chemoselective formation of *C*- and *N*-terminal oximes resulting in a mixture of four isomeric forms due to *syn–anti* isomerism of the oxime bonds. Some isomers could be monitored by HPLC and identified by NMR. The molecule containing a naphthalene-derived template was found to inhibit the VCAM-1/VLA-4 interaction more efficiently than previously reported for sulfur-bridged cyclic peptides containing similar sequences. The finding confirms the importance of incorporating conformational constraints between the terminal ends of the peptide loop **37–43** in the design of synthetic inhibitors of the VCAM-1/integrin interaction.

Keywords: VCAM-1 mimetics; template assembly; constrained cyclic peptides; chemoselective ligation; drug design

INTRODUCTION

The main goal in protein mimicry is to reproduce the receptor, sensory, and catalytic functions of proteins in smaller molecules accessible by chemical synthetic methods or by recombinant techniques [1–5]. Proteins have been successfully reduced in size by a combination of random mutagenesis and a selection method based on phage display techniques as well as chemical synthesis [6–8]. These protein mimetics represent versatile models for the investigation of the complex structure–function relationship in proteins. Moreover, if a protein can be reduced to a size easily accessible by chemical synthesis, a variety of non-natural architectures and non-proteinogenic amino acids can be introduced.

In an alternative approach, small, conformationally stable protein domains have been used as scaffolds for grafting binding loops of native proteins and receptors [9–14]. Here, attached loops are randomly exchanged by mutagenesis to provide a library of conformationally defined proteins.

The Template Assembled Synthetic Proteins (TASP) concept has been introduced [15] to overcome the main hurdle in protein *de novo* design, i.e.

Abbreviations: Alloc, allyloxycarbonyl; BCECF-AM, 2′,7′-bis-(2-carboxyethyl)-5(and-6)-carboxyfluorescein-acetoxymethylester; Boc, *tert*-butoxycarbonyl; BSA, bovine serum albumin; Dap, α,β-L-diaminopropionic acid; DCM, dichloromethane; DIPEA, diisopropylethylamine; DMF, *N*,*N*-dimethylformamide; DMSO, dimethylsulfoxide; Fmoc, 9-fluorenylmethoxycarbonyl; IgSF, immunoglobulin superfamily; *t*Bu, *tert*-butyl; TIS, tris-isopropylsilane; Trt, trityl; PBS, phosphate buffered saline; PyBOP, benzotriazole-yl-oxy-tris-pyrrolidino-phosphonium hexafluorophosphate; VCAM-1, vascular cell adhesion molecule-1; VLA-4, very-late antigen-4.

* Correspondence to: Institute of Organic Chemistry, University of Lausanne, BCH-Dorigny, CH-1015 Lausanne, Switzerland. E-mail: Manfred.Mutter@ico.unil.ch

Contract/grant sponsor: Swiss National Science Foundation
Contract/grant sponsor: Novartis Pharma AG (Basel)

CCC 1075–2617/99/070313-10$17.50

the protein folding problem. In a recent extension of this approach, the functional part of a protein is detached from the rest of the molecule and assembled on a topological template, mimicking the structural framework of the native protein. Secondary structure elements such as α-helices or loops have been assembled on regioselectively addressable templates [16–21].

Here, we describe the design, synthesis and biostructural characterization of constructs containing an integrin-binding loop grafted onto aromatic templates as functional mimetics of the Vascular Cell Adhesion Molecule 1 (VCAM-1) protein.

MATERIALS AND METHODS

All protected amino acids were purchased from Calbiochem-Novabiochem (Läufelfingen, Switzerland). Reagents and solvents were purchased from Fluka (Buchs, Switzerland) and used without further purification. HPLC was performed on Waters equipment using a column packed with Vydac Nucleosil 300 Å 5 μm C_{18} particles unless otherwise stated. The analytical column (250 × 4.6 mm) was operated at 1 ml/min and the preparative column (250 × 21 mm) at 18 ml/min, monitoring at 214 nm. Solvent A consisted of 0.09% TFA in water and solvent B of 0.09% TFA in acetonitrile/water 9:1. Mass spectra were obtained by electron spray ionization (ESI-MS) on a Finningan MAT SSQ 710C. NMR spectra were recorded in H_2O/D_2O (9:1, v/v) at 400 MHz using a Bruker ARX spectrometer at 300 K. Water signal suppression was accomplished using the WATERGATE pulse sequence. Two-dimensional experiments were typically acquired using 2K × 512 matrices over a 2000 Hz sweep width in both dimensions. Quadrature detection in the indirect dimension was achieved by using the TPPI procedure. Scalar connectivities were recovered from two-dimensional double quantum filtration (DQF) COSY experiments. Dipolar connectivities were obtained either through the conventional NOESY sequence or the ROESY sequence with mixing times from 150 to 200 ms. A randomization of the mixing length ($\pm$ 5%) was introduced in the NOESY experiments in order to minimize coherence transfer. The spin lock mixing interval of the ROESY sequence was applied by coherent CW irradiation at $\gamma B_2/2\pi = 1$ kHz. Experimental data processing was performed using the Felix software package. The standard sinebell squared routine was employed for apodization with a shift range of 60–90° and zero filling in both dimensions before two-dimensional transformations were applied to end up with square matrices of 2K × 2K real point data.

Peptide Solid-Phase Synthesis

Peptides were synthesized manually following a standard Fmoc solid-phase synthetic protocol [22–24]. The resin was swollen in DCM for about 30 min before starting the synthesis. Commercial DMF was degassed for several hours with nitrogen. In the coupling steps, *N*(α)-Fmoc amino acid (1.5 equivalents) activated in situ with PyBOP (1.5 equivalents) in the presence of DIPEA (3 equivalents) were used. The *N*(α)-Fmoc deprotection was carried out by treatment with piperidine (20% v/v in DMF, 1 × 5 min and 2 × 10 min) and assessed by UV analysis (at $\lambda = 301$ nm) of the effluents. The *N*(α)-Fmoc amino acids were protected at the side chains functional groups as follows: *tert*-Butyl for Thr, Asp and Ser and Trityl for Gln.

Peptide Sequence with Aminooxy Linkers

The sequence Thr(*t*Bu)-Gln(Trt)-IleAsp(OtBu)-Ser(*t*Bu)-Pro-Leu-Dap(*N*(α)-Alloc)- was assembled on Rink Amide MBHA resin (loading: 0.4 mmol/g) using the Fmoc strategy described above. The *N*(α)-Alloc-*N*(β)-Fmoc-diaminopropionic acid was linked to the resin and its *N*(α)-amino group provided the *C*-terminal attachment site for the aminoxyacetyl moiety. After removal of the Alloc group ($PhSiH_3$, 24 equivalents; $Pd(PPh_3)_4$, 0.10 equivalents in DCM under argon, 10 min [25]), two aminoxyacetyl moieties were linked at the α-amino groups of Thr and Dap by reacting the peptide resin with *N*-Boc aminoxyacetyl hydroxysuccinimide (3 equivalents) in the presence of DIPEA (6 equivalents) in DMF (30 min, room temperature [r.t.]). The cleavage from the resin and complete deprotection by treatment with a TFA/H_2O/TIS mixture (95, 2.5, 2.5%, v/v), afforded peptide **IV**.

Naphthalene Tetraethyl-diacetal (2,7-Di-(1′,1′-bis(ethoxy)ethyloxy)-naphthalene)

The 2,7-dihydroxynaphthalene (**I**) ($M_r = 160$, 5 mmol, 800 mg) was dissolved in dry DMF (20 ml); the bromoacetaldehyde diethylacetal ($M_r = 197$, $d =$ 1.27, 10 equivalents, 7.8 ml) and the Cs_2CO_3 ($M_r =$ 325.8, 4 equivalents, 6.5 g) were added. The heterogeneous solution was refluxed for 24 h at 70°C under nitrogen and with vigorous stirring.

After *in vacuo* evaporation of the solvent, the residue was taken up with ethyl acetate (100 ml) and extracted with saturated $NaHCO_3$ (two times, 100 ml) and brine (two times, 150 ml). The organic phase was dried over Na_2SO_4 and evaporated to dryness. The crude was purified by flash chromatography on silica gel (eluent: hexane/ethyl acetate = 7:3), recrystallization from diethyl ether gave the diacetal as a white powder (52% yield). ^{1}H-NMR (400 MHz, $CDCl_3$): δ (ppm) = 1.28 (t, 12H, CH_3, $J = 7.0$ Hz), 3.65 (dq, 4H, $-O-CH_2-CH_3$, $J_d = 9.3$ Hz, $J_q = 7.0$ Hz), 3.81 (dq, 4H, $-O-CH_2-CH_3$, $J_d = 9.3$ Hz, $J_q = 7.0$ Hz), 4.12 (d, 4H, Ar–O–CH_2–, $J = 5.2$ Hz), 4.90 (t, 2H, $CH(OEt)_2$, $J = 5.2$ Hz), 7.0 and 7.6 (m, 6H, H_{arom}) MS: $m/z = 392$ (M), 347 (M-45), 301 (M-91), 255 (M-137).

Dialdehyde II (2,7-Di-formylmethoxy-naphthalene)

A solution of the tetraethyl-diacetal ($M_r = 392$, 5 mmol, 1.96 g) in acetic acid and 1 N HCl (50 ml, 50%, v/v) was stirred at r.t. for 30 min, then solvents were evaporated *in vacuo*, the residue was redissolved in the same solvent mixture and stirred for other 30 min at r.t.; reaction/solvent evaporation cycles were repeated until the tetraacetal was completely hydrolysed to aldehyde as judged from TLC (eluent: chloroform/MeOH = 9:1 v/v). Solvents were then removed and the residue was taken up with ethyl acetate (50 ml), washed with aqueous bicarbonate, dried on sodium sulfate, filtered and concentrated. Compound **II** was recovered as a white powder (1.16 g, 95% yield) and almost immediately reacted with the hydroxylamino-peptide **IV**. ^{1}H-NMR (400 MHz, $CDCl_3$): δ (ppm) = 4.67 (s, 4H, Ar–O–CH_2), 7.0 and 7.6 (m, 6H, H_{arom}). MS: $m/z = 244$ (M). Anal. Calc. for $C_{14}H_{12}O_4$: C 68.8, H 4.9; found C 67.9, H 5.3.

Biphenyl Tetraethyl-diacetal (2,2′-Di-(1″,1″-bis(ethoxy)ethoxy) × -5,5′-dimethyl-biphenyl)

The 2,2′-dihydroxy-5,5′-dimethyl-biphenol was synthesized as previously reported [26] and transformed in the tetraethyl-diacetal as described for the 2,7-dihydroxynaphthalene with a yield of 75% on purified product. ^{1}H-NMR (400 MHz, $CDCl_3$): $\delta = 1.10$ (t, 12H, CH_3, $J = 7.0$ Hz), 2.30 (s, 6H, CH_3–Ar), 3.40 (dq, 4H, $-O-CH_2-CH_3$, $J_d = 9.3$ Hz, $J_q = 7.0$ Hz), 3.59 (dq, 4H, $-O-CH_2-CH_3$, $J_d = 9.3$ Hz, $J_q = 7.0$ Hz), 3.89 (d, 4H, Ar–O–CH_2–, $J = 5.2$ Hz), 4.58 (t, 2H, $CH(OEt)_2$, $J = 5.2$ Hz), 6.8 and 7.0 (m, 6H, H_{arom}). MS: $m/z = 446$ (M), 309 (M-137).

Biphenyl Dialdehyde (2,2′-Di-formylmethoxy-5,5′-dimethyl-biphenyl)

The biphenyl tetraethyl-diacetal was hydrolysed to the dialdehyde as described for **II**. ^{1}H-NMR (400 MHz, $CDCl_3$): $\delta = 2.34$ (s, 6H, CH_3-aryle), 3.89 (s, 4H, Ar–O–CH_2), 6.8 e 7.0 (m, 6H, H_{arom}). Mass: $m/z = 298$ (M). Anal. Calc. for $C_{18}H_{18}O_4$: C 72.5, H 6.0; found C 73.1, H 5.7.

General Procedure for Coupling Peptide IV to Templates

To a 0.5 mM solution of **IV** in aqueous acetate buffer (0.05 M, pH 4)/DMF (1:1, v/v), 1.1 equivalents of dialdehyde was added; the solution was stirred at r.t., following the cyclization by analytical HPLC. The reaction was generally complete after 1 h and pure products were recovered by evaporating the solvent in vacuo and by purifying by preparative HPLC.

Compound 1. After 1 h of cyclization at r.t. and solvent evaporation, the pure compound **1** was purified as a mixture of four isomers by preparative HPLC (5–95% solvent B over 30 min). Product characterization by analytical HPLC (from 20 to 50% of B in 30 min): $R_t = 13.0$, 14.4, 15.3 and 16.0 min for the four isomeric peaks. ESI-MS: $m/z = 626.2$ (M + 2/2), 1212.9 (M), 1235.1 (M + 23[Na]).

Compound 2. Analytical HPLC (from 20 to 50% of B in 30 min): $R_t = 20.0$, 20.7, 20.9 min for the four scarcely resolved peaks. ESI-MS: $m/z = 1266.5$ (M).

Compound 3. The peptide was cyclized on the commercially available isophthalaldehyde following the same procedure described for compounds **1** and **2**. Analytical HPLC (from 20 to 50% of B in 30 min): $R_t = 11.5$ min. ESI-MS: $m/z = 1102.9$ (M).

Compound 4. A solution of peptide **IV** ($M_r = 1004$, 20 mg, 0.02 mmol) and benzaldehyde ($M_r = 106$, $d = 1.05$, 4 μl, 1 equivalent) in 10 ml of DMF/acetate buffer pH 4 (50%, v/v) was stirred at r.t. for 1 h. After solvent evaporation, the residue was purified by HPLC (5–95% of B in 30 min). Analytical HPLC (from 20 to 50% of B in 30 min): $R_t = 20.0$ min. ESI-MS: $m/z = 1180.1$ (M).

Cell Adhesion Assays

Microtiter plates (Maxisorb, Nunc) were coated with 3 μg/ml goat anti-mouse IgG-κ chain antibody (SBA, Birmingham, USA) in 15 mM sodium bicarbonate buffer (pH 8.7) at 4°C overnight. The coating solu-

tion was removed and plates were blocked with 3% BSA (Fluka) in PBS at 37°C for 2 h. The plates were washed once with 50 mM Tris–HCl (pH 7.4) containing 150 mM NaCl, 5 mM glucose, 3 mM $MnCl_2$ and 0.5% BSA (binding buffer) followed by the addition of 0.1 μg/ml recombinant VCAM-1 mouse Cκ fusion protein in binding buffer. The VCAM-1 mouse Cκ fusion protein was produced as described for recombinant E-selectin mouse Cκ fusion protein [27]. After incubation at 37°C for 2 h plates were washed three times with binding buffer. Ramos cells (ATCC) were cultured in RPMI 1640 supplemented with 10% fetal calf serum, 2 mM glutamine and non-essential amino acids (Gibco). Cell density was kept below $1.3 \cdot 10^6$ cells/ml. The cells were fluorescently labeled in binding buffer containing 10 μg/ml BCECF-AM (Molecular Probes) at 37°C for 45 min and washed once in binding buffer.

Peptides dissolved in water or DMSO were diluted in binding buffer and added at twice their final desired concentration (50 μl/well). Then $1 \cdot 10^5$ labeled Ramos cells in 50 μl binding buffer were added to each well. After an incubation at r.t. for 30 min unbound cells were removed by aspiration using a SIGMA 12-well harvester comb (M-2781). The wells were washed two times with binding buffer. Bound cells were quantified by measuring fluorescence using a Cytofluor 2350 (Millipore) at E_x/E_m: 485 nm/530 nm.

Computational Procedure for Molecular Dynamics

All modeling studies were performed with the molecular graphics package INSIGHT (version 2.9.6; Molecular Simulations, 1993). Energy minimization and molecular dynamics simulations were achieved on a Silicon Graphics IndigoII using the program CVFF/DISCOVER (version 2.9; Molecular Simulations, 1993). Minimization procedures consisted of 200 steps steepest descent, followed by a conjugate gradient minimization until the r.m.s. gradient was < 0.01 kcal/mol Å. For all calculations a distance-dependent dielectric term ($\varepsilon = 4.00r$) approximating aqueous surrounding was chosen. A low energy starting conformation of each molecule was found, by connecting the template/linker to the peptide sequence and performing a molecular dynamics run of 100 ps at 600 K, whereas the coordinates of the loop were kept fixed. The structure with lowest energy was used as starting structure for the unrestrained dynamics simulation. The dynamics runs were performed by using standard DISCOVER protocols at a constant temperature of 300 K. After 10 ps initialization time the system was then subjected to a 500 ps simulation time. Structures were saved every 5 ps and energy minimized. The average structures were generated by INSIGHT and once more energy minimized.

RESULTS AND DISCUSSION

Design of VCAM-1 Mimetics

The crystallization of the integrin-binding domain of VCAM-1 [28], a protein belonging to the immunoglobulin superfamily (IgSF) along with extensive mutagenesis studies [29,30] have provided a detailed understanding of the integrin-binding sites, revealing essential residues (e.g. Asp^{40}). Most notably, the CD-loop **37**–**43**, Thr-Gln-Ile-Asp-Ser-Pro-Leu, plays a crucial role for the biological activity of the protein. The three-dimensional structure of the CD-loop is stabilized by three internal hydrogen bonds and additional hydrogen bonds to the EF-loop [31]. One of the internal hydrogen bonds is formed by the Thr^{37} carbonyl and the Asp^{40} amino group, inducing a β-turn on the corner of the CD-loop in which the important residue Asp^{40} is located at the $i+3$ position. Pro^{42} appears to be particularly important, since its limited conformational freedom brings the Cα atoms of Thr^{37} and Leu^{43} within 7 Å.

The *N*-terminal portion of the CD-loop provides a structurally distinct motif for the IgSF/integrin class of adhesion interactions. This folding motif may occur more generally in integrin-binding molecules, as the related sequence motif Leu-Asp-Val has been shown to be essential for very-late antigen-4 (VLA-4) mediated cell adhesion by the alternatively spliced type-III connecting segment domain of fibronectin. The tripeptide segment Arg-Gly-Asp (RGD) plays a role in mediating binding for a range of molecules that interact with the non-leukocyte integrins. RGD containing peptides are potent competitors of the integrin binding, one of these inhibiting the VCAM-1/VLA-4 interaction [32]. However, the conformation of the CD-loop in VCAM-1 shows little similarity to the RGD structure as observed in various integrin-binding proteins, featuring a highly exposed, negatively charged side chain located in a flexible loop region. Such side chains may contribute to adhesion by completing a divalent cation-binding site in the integrin.

The binding loop (**37**–**43**) of the first VCAM-1 domain is assembled onto aromatic templates, which substitute the loop supporting structural

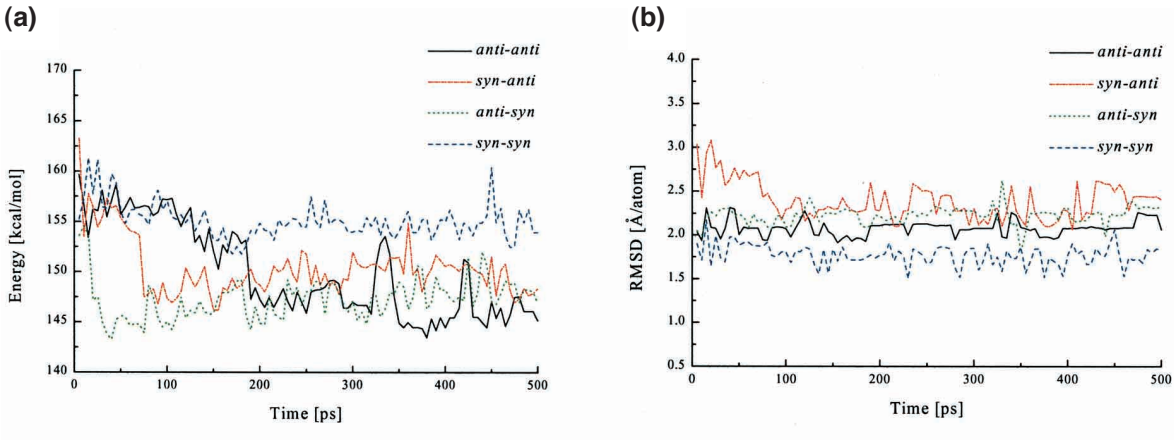

Plate 1 Evolution of the energy for naphthalene/linker system (a) and of RMSD values for peptide backbone (b) calculated for the four oxime isomers of compound **1** (see text).

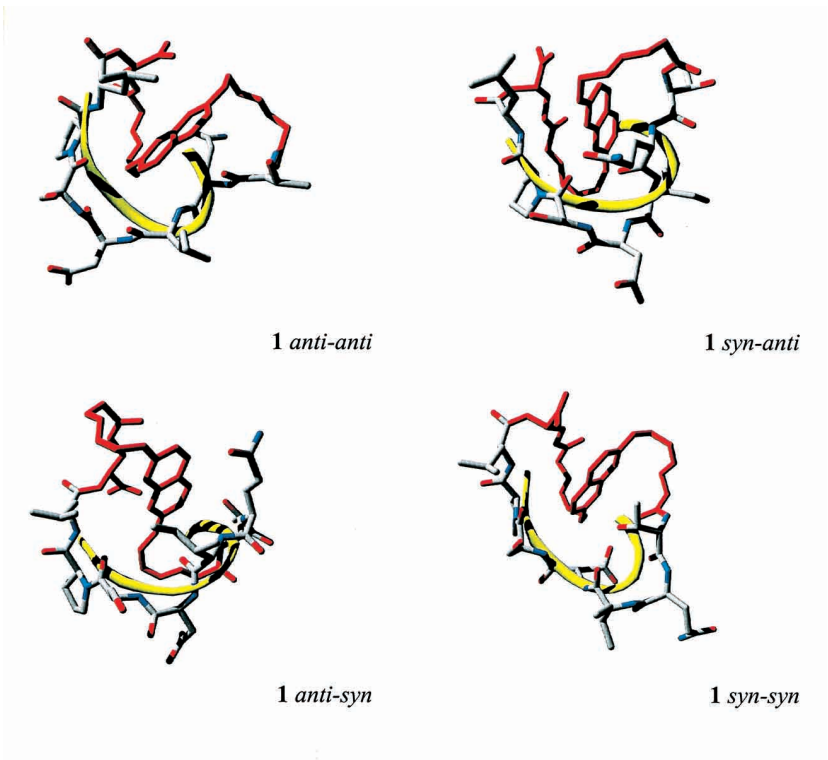

Plate 2 Stick representation of averaged structures of **1** (template red) superimposed on to the backbone ribbon (yellow) of the X-ray structure. Hydrogen atoms are omitted for clarity.

framework of the native protein (Figure 1). A cyclic, disulfur-bridged peptide containing the shorter sequence (**37–42**) was proved to be active in inhibiting the VLA-4/VCAM-1 interaction [33], while its linear analog was found to be completely inactive.

The naphthalene- (**1**), biphenyl- (**2**) and phenyl-derived (**3**) templates were evaluated for their propensity to constrain the VCAM-1 (**37–43**) peptide in a native-like conformation by molecular dynamics simulations.

Synthesis

Compounds **1–4** (Figure 1) were prepared according to convergent strategies (Scheme 1) applying chemoselective condensation in the solution of the dioxyaminoacetyl-peptide (**IV**) with a dialdehyde template (**II**). This synthetic pathway is particularly suitable for functional screening of different templates linked to identical peptide fragments.

The VCAM-1 sequence (**37–43**) was assembled by stepwise solid phase synthesis using Fmoc chemistry, thus obtaining peptide **III**; the *C*-terminal *N*(α)-Alloc-Dap residue was directly linked to the Rink-Amide MBHA resin, providing an amino functionality at the *C*-terminal end of the peptide. After removal of the Alloc group (step **c**), two *N*-Boc-aminooxyacetyl moieties were coupled in solid phase to the α-amino groups of Thr and Dap (step **d**), thus providing the *N*-terminal aminooxy functional groups for chemoselective ligation [34–36]. After cleavage and deprotection (step **e**), peptide **IV** was condensed to the functional template **II** in DMF/aqueous buffer at pH 4 (step **f**), thus affording mimetic **1**. The cyclization reactions (oxime bond formation) were followed by analytical HPLC and proceeded in good yields giving compounds **1–3** without detectable side product formation. In the case of linear peptide **4**, the aminooxy ends of **IV** were capped by reacting with 2 equivalents of benzaldehyde.

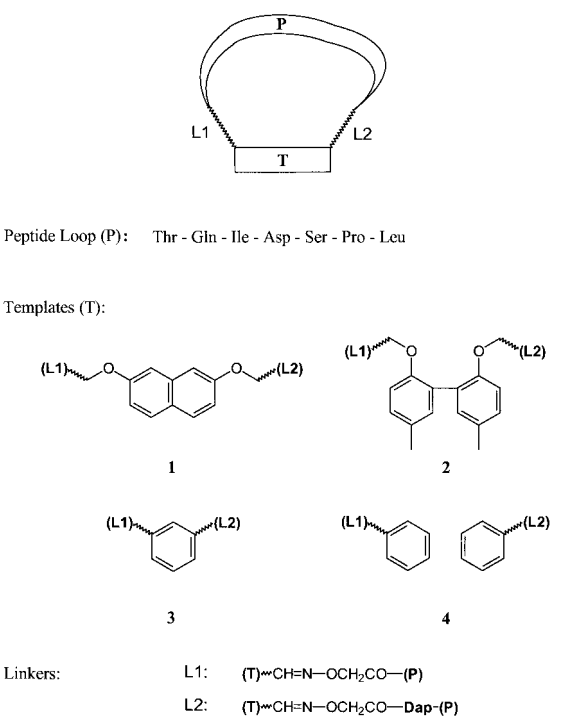

Figure 1 VCAM-1 mimetics **1–4**.

Characterization

The HPLC profiles of compounds **1–3** showed at r.t. and under identical gradient conditions four well-resolved peaks for **1**, partially overlapping peaks for **2** and one single peak in the case of **3** and **4** (Figure 2).

The HPLC peaks of **1** and **2** were found to correspond to four constitutional isomers[1], originating in the combinations of *syn* and *anti* configurations of the two oxime bonds. The presence of an equilibrium of *syn–syn*, *syn–anti*, *anti–syn* and *anti–anti* isomers was confirmed by ^{1}H-NMR analysis. The ^{1}H-NMR spectra of **1–4**, recorded in aqueous solution (10% D_2O in H_2O) at pH 5.0 and 300 K, showed for each compound that the two oxime C–H protons (H-1 and H-2) resonate as two singlets corresponding to the *syn* and the *anti* configurations of the carbon–nitrogen double bond (in the case of **3**: 6.7 ppm, H-1_{syn}, 7.4 ppm, H-1_{anti}; 7.2 ppm, H-2_{syn} and 7.6 ppm, H-2_{anti}). Chemical exchange between the signals corresponding to the *syn* and *anti* configuration of compounds **1–4** was ascertained in ROESY spectra from cross-peaks having the same phase as the diagonal. For compounds **3** and **4**, the presence of one set of sharp signals is indicative of a fast chemical exchange regime. These findings are consistent with the HPLC profiles at r.t., i.e. four separated conformers in **1** and **2**, while averaging is observed for **3** and **4**.

The ratio of the four isomers of **1** (56:13:24:5), calculated from the peak integration of HPLC chromatograms, did not change significantly in raising the temperature to 70°C in water at pH 6, indicating an enthalpically driven equilibrium. The isomers of **1** were isolated by HPLC (gradient 20–50% solvent B in 40 min) and the fractions containing pure isomers were reinjected, showing a single peak pattern. After 1 h at r.t., each reequilibrated isomer is

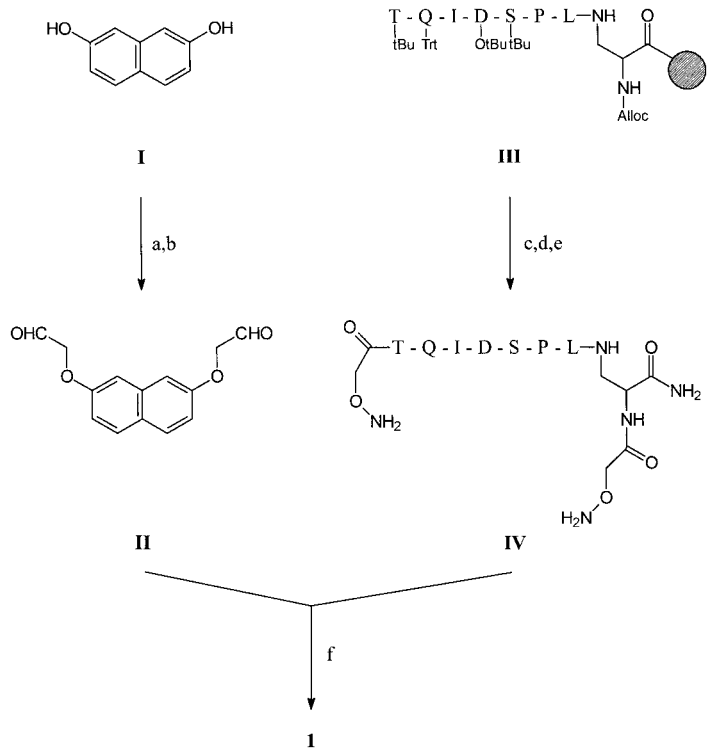

Scheme 1 Convergent strategy for the synthesis of VCAM-1 mimetic **1**. (a) $BrCH_2CH(OEt)_2$ (10 equivalents), Cs_2CO_3 (4 equivalents), DMF, 70°C, 24 h. (b) AcOH/HCl 1 N, 1 h, removal of EtOH *in vacuo*; **II**: 34% yield. (c) Solid-phase synthesis of peptide **III** on Rink amide resin using Fmoc strategy, then Alloc cleavage with $Pd(PPh_3)_4$ (0.10 equivalents), $PhSiH_3$ (24 equivalents), in DCM, 10 min, r.t. (d) Boc-NH-O-CH_2-COOSu (3 equivalents), DIPEA (6 equivalents), DMF, 30 min, r.t. (e) TFA 95%, TIS 2.5%, H_2O 2.5%, 1 h, r.t.; **IV**: 65% yield. (f) Peptide **IV**, $5 \cdot 10^{-4}$ M in 50% DMF/acetate buffer (pH 4) (1:1, v/v) and dialdehyde **II** (1.1 equivalents), 1 h, r.t.; **1**: 89% yield.

showing the identical HPLC profile composed of four peaks.

Compounds **1**–**4** were tested for inhibition of VCAM-1/VLA-4 dependent adhesion by *in vitro* binding assays. Only compound **1** was found to be active at $IC_{50} \approx 0.4$ mM[2]. The binding curves of the mimetics, compared to the one of the disulfur-bridged peptide *c*(Cys-Gln-Ile-Asp-Ser-Pro-Cys) [33] are shown in Figure 3. These experimental data confirm that the presence of the naphthalene template between the terminal residues of the loop enhances the activity of the synthetic inhibitor, thus encouraging the use of rigid templates in the design of these types of protein loop mimetics.

Molecular Dynamics Simulation

The impact of the constraint imposed by the template upon the backbone and side-chain conformations was estimated by molecular dynamics simulations. Using the X-ray structure of the CD-loop domain of VCAM-1 as the starting point for the calculations[3], the time-dependent evolution of the loop structure at r.t. was followed. As the R–O–N=C connectivity of the oxime bonds was not parameterized for any known force field, the values for the R–O–C=C group were taken as a first approximation. All four isomers of the oxime bond in cyclic compounds **1**–**3** (*syn–syn*, *syn–anti*, *anti–syn*, *anti–anti*) were treated separately in the simulations. In order to explore a broad region of the conformational space, a long simulation time (500 ps) was chosen. After a period of 150 ps, the peptidic parts of molecules **1**–**3** were relaxed and did not change its conformation significantly; structural changes were principally observed in the linker part of the molecules. This became obvious by comparing the fluctuation of the calculated energies for the template/linker part with the RMSD values of the backbone of the peptidic part, as shown in Plate 1 for the four isomers of **1**.

Four different minimized structures were obtained for each cyclic compound, corresponding to the four combinations of the *syn* (E) and *anti* (Z)

forms of the two oxime bonds as presented in Plate 2 for compound **1**. As a common feature of these structures[4], the peptide part shows generally a good superposition with the corresponding loop of the native protein, whereas the template/linker part forms a compact hydrophobic core surrounded by the loop.

From the series of VCAM-1 mimetics **1**–**3**, preliminary conclusions on structure–function correlations can be drawn. The linear peptide **4** being rather flexible in solution and lacking any spatial pre-organization of functional groups, turns out to be completely inactive despite the presence of the potentially active sequence. In mimetics **1**–**3**, the templates reduce dramatically the conformational space of the molecules. The observed activity of compound **1** may originate from the rigidity of the naphthalene-based spacer resulting in a fixed distance between the *C*- and the *N*-terminal residues of the loop. The average distance between the *Nα* of Thr^{37} and CO carbon of Leu^{43} was found to be ≈ 10 Å in the minimized structures of the *syn–anti* and *anti–syn* isomers of **1**, and ≈ 11 Å for the *syn–syn* and the *anti–anti* forms, respectively. These values are significantly larger compared to the native protein loop (7.36 Å), indicating that a redesign of the linker group could result in increased binding affinity. The $d_{NH_{37}-CO_{43}}$ values for the minimized structures of **2** have a broad fluctuation range, varying from 5.5 Å for the *syn–syn* to 12.6 Å of the *anti–syn* isomer. Here, the overall mobility is probably too high to ensure a conformational 'lock-in' of the peptide in an appropriate conformation. In compound **3**, the distance between *C*- and *N*-terminal residues of the loop is about 8.5 Å (averaged on the four isomeric forms), being comparable to that of the native protein. Deviations of the distance $d_{NH_{37}-CO_{43}}$ values are all less than 10% during the simulations of **1**–**3**.

CONCLUSIONS

The effect of aromatic templates upon the loop structure of mimetics **1**–**4** (Figure 1) is studied by evaluating the *in vitro* activity in inhibiting the

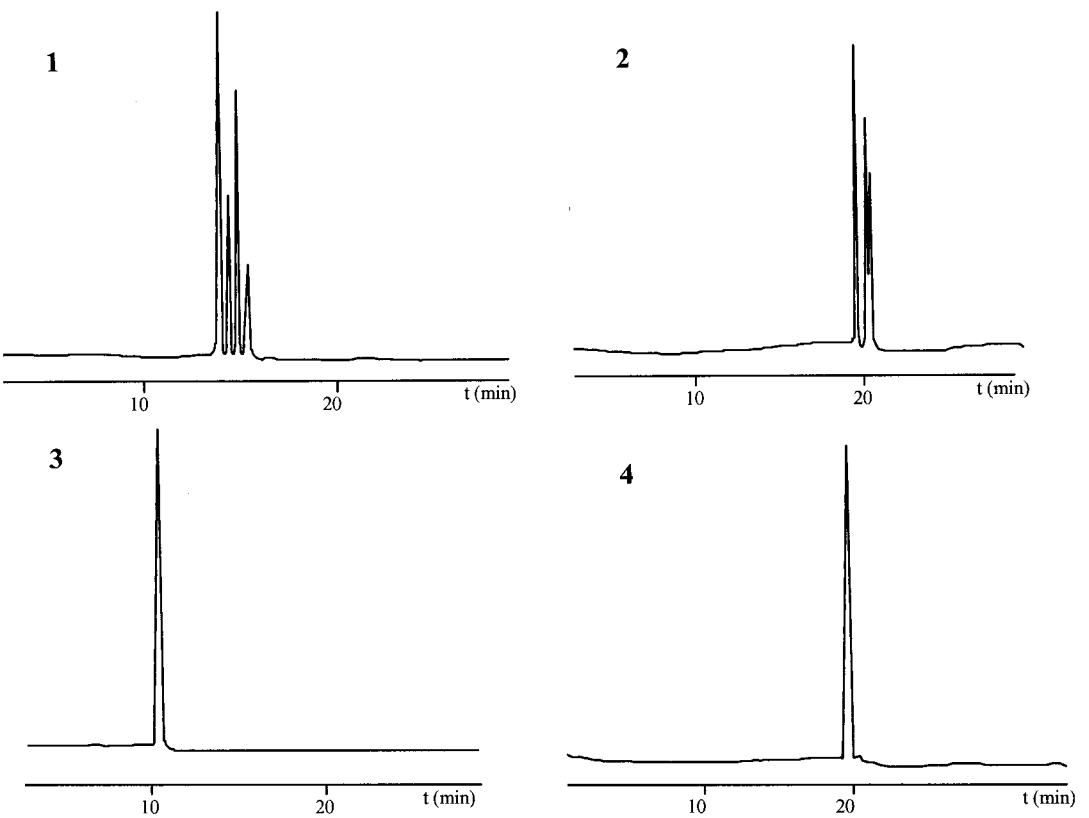

Figure 2 HPLC profiles of compounds **1**–**4** at r.t. (gradient: 20–50% of B in 30 min); **1**, $R_t = 13.0$, 14.4, 15.3 and 16.0 min; **2**, $R_t = 20.0$, 20.7, 20.9 min; **3**, $R_t = 11.5$ min; **4**, $R_t = 20.0$ min.

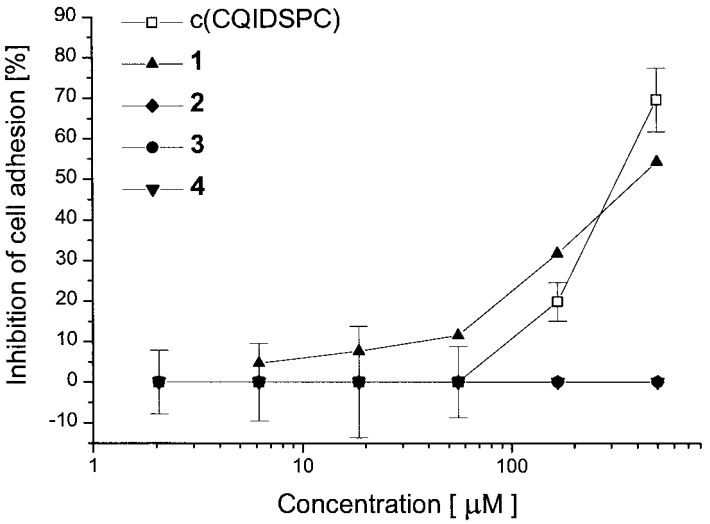

Figure 3 Effect of synthetic VCAM-1 mimetics **1**–**4** and S–S bridged Cys-Gln-Ile-Asp-Ser-Pro-Cys (*c*[CQIDSPC]) on the adhesion of Ramos cells to recombinant VCAM-1. Ramos cells were allowed to adhere to immobilized VCAM-1 in the presence of mimetics **1**–**4** as described. Each point represents the mean ± S.D. of triplicates.

VCAM-1/VLA-4 ($\alpha_4\beta_1$) specific recognition. A detailed understanding of the interaction between VLA-4 and VCAM-1 recognition sites [37–39] represents an important starting point for the design and development of putative anti-inflammatory drugs. The biological activity of **1** makes this molecule an interesting lead compound for structural optimization applying combinatorial approaches, although its activity cannot be assigned or attributed to one single isomer. Molecular dynamics simulations reveal the effect of the template on the preferred loop conformations. Consequently further structural modifications of the templates represent a reasonable starting point in future structure–function studies.

The studies presented here show the potential of the template concept to stabilize exposed loops in proteins. Investigations for optimizing the bioactivity of compound **1** applying combinatorial methods are in progress.

Acknowledgements

We gratefully acknowledge the Swiss National Science Foundation and Novartis Pharma AG (Basel) for financial support.

NOTES

1. Compounds **1** and **2** were analysed with a LC/ESI-MS instrument and for each compound the different peaks revealed the same mass ($M_r = 1212.9$ for **1** and $M_r = 1266.5$ for **2**). Compounds **3** and **4** showed a single peak at various gradients condition in the RP-HPLC analysis.
2. Ramos cells were allowed to adhere to immobilized VCAM-1 in the presence of peptides as described in the 'Materials and Methods'. In two different experiments (each one in triplicate), IC_{50} values of 0.3 and 0.54 mM were found for compound **1**.
3. Coordinates of the X-ray structure of VCAM-1 were obtained from the Brookhaven Crystallographic Database PDB code: 1vsc.
4. The same type of calculations were run for molecules **2** and **3** giving a good superposition of the peptide part with the native-protein loop for both molecules.

REFERENCES

1. Mutter M, Tuchscherer G. Non-native architectures in protein design and mimicry. *Cell Mol Life Sci* 1997; **53**: 851–863.
2. Bryson JW, Betz SF, Lu HS, Suich DJ, Zhou HXX, O'Neil KT, DeGrado WF. Protein design — a hierarchical approach. *Science* 1995; **270**: 935–941.

3. Baltzer L. Functionalization of designed folded polypeptides. *Curr Opinion Struct Biol* 1998; **8**: 466–470.
4. Rau HK, Dejonge N, Haehnel W. Modular synthesis of *de novo* designed metalloproteins for light-induced electron transfer. *Proc Natl Acad Sci* USA 1998; **95**: 11526–11531.
5. Tuchscherer G, Schleibler L, Dumy P, Mutter M. Protein design: on the threshold of functional properties. *Biopolymers* 1998; **47**: 63–73.
6. Braisted AC, Wells JA. Minimizing a binding domain from protein A. *Proc Natl Acad Sci USA* 1996; **93**: 5688–5692.
7. Cunningham BC, Wells JA. Minimized proteins. *Curr Opinion Struct Biol* 1997; **7**: 457–462.
8. Struthers MD, Cheng RP, Imperiali B. Economy in protein design: evolution of a metal-independent motif based on the zinc finger domains. *J Am Chem Soc* 1996; **118**: 3073–3081.
9. Pessi A, Bianchi E, Crameri A, Venturini S, Tramontano A, Sollazzo M. A designed metal-binding protein with a novel fold. *Nature* 1993; **362**: 367–369.
10. Vita C, Vizzavona J, Drakopoulou E, Zinn-Justin S, Gilquin B, Menez A. Novel miniproteins engineered by the transfer of active sites to small natural scaffolds. *Biopolymers* 1998; **47**: 93–100.
11. Nygren PA, Uhlen M. Scaffolds for engineering novel binding sites in proteins. *Curr Opinion Struct Biol* 1997; **7**: 463–469.
12. Vita C, Roumestand C, Toma F, Menez A. Scorpion toxins as natural scaffolds for protein engineering. *Proc Natl Acad Sci USA* 1995; **92**: 6404–6408.
13. Perez-Paya E, Houghten RA, Blondelle SE. Functionalized protein-like structures from conformationally defined synthetic combinatorial libraries. *J Biol Chem* 1996; **271**: 4120–4126.
14. Houston ME, Wallace A, Bianchi E, Pessi A, Hodges RS. Use of a conformationally restricted secondary structural element to display peptide libraries: a two stranded alpha helical coiled-coil stabilized by lactam bridges. *J Mol Biol* 1996; **262**: 270–282.
15. Mutter M, Vuilleumier S. A chemical approach to protein design: Template Assembled Synthetic Proteins (TASP). *Angew Chem Int Ed Engl* 1989; **28**: 535–554.
16. Mutter M, Tuchscherer G, Miller C, Altmann KH, Carey RI, Wyss DF, Labhard AM, Rivier JE. Template-assembled synthetic proteins with four-helix-bundle topology. Total chemical synthesis and conformational studies. *J Am Chem Soc* 1992; **114**: 1463–1470.
17. Mutter M, Dumy P, Garrouste P, Lehmann C, Mathieu M, Peggion C, Peluso S, Razaname A, Tuchscherer G. Template assembled synthetic proteins (TASP) as functional mimetics of proteins. *Angew Chem Int Ed Engl* 1996; **35**: 1482–1485.
18. Sila U, Mutter M. Topological templates as tool in molecular recognition and peptide mimicry: Synthesis of a TASK library. *J Mol Recognition* 1995; **8**: 2934.
19. Bisang C, Weber C, Robinson JA. Protein-loop mimetics: a diketopiperazine-based template to stabilize loop conformations in cyclic peptides containing the NPNA and RGD motifs. *Helv Chim Acta* 1996; **79**: 1825–1842.
20. Beeli R, Steger M, Linden A, Robinson JA. A tricyclic template derived from (2*S*,4*R*)-4-hydroxyproline for the synthesis of protein loop mimetics. *Helv Chim Acta* 1996; **79**: 2235–2248.
21. Emery F, Bisang C, Favre M, Jiang L, Robinson JA. A template for the solid-phase synthesis of conformationally restricted protein loop mimetics. *Chem Commun* 1996; 2155–2156.
22. Fields GB, Noble RL. Solid phase peptide synthesis utilizing 9-fluorenylmethoxycarbonyl amino acids. *Int J Pept Protein Res* 1990; **35**: 161–214.
23. Sheppard RC. Continuous flow methods in organic synthesis. *Chem Brit* 1983; 402.
24. Chang CD, Meienhofer J. Solid-phase peptide synthesis using mild base cleavage of $N\alpha$-fluorenylmethyloxycarbonylamino acids, exemplified by a synthesis of dihydrosomatostatin. *Int J Pept Protein Res* 1978; **11**: 246–249.
25. Thieret N, Alsina J, Giralt E, Guibé F, Albericio F. Use of Alloc-amino acids in solid-phase peptide synthesis-tandem deprotection-coupling reactions using neutral conditions. *Tetrahedron Lett* 1997; **41**: 7275–7278.
26. Sartori G, Maggi R, Bigi F, Arienti A, Casnati G. Regiochemical control in the oxidative coupling of metal phenolates: highly selective synthesis of symmetric, hydroxylated biaryls. *Tetrahedron* 1992; **48**: 9483.
27. Weitz-Schmidt G, Stokmaier D, Scheel G, Nifant'ev NE, Tuzikov AB, Bovin NV. An E-selectin binding assay based on a polyacrymide-like glycoconjugate. *Anal Biochem* 1996; **238**: 184–190.
28. Jones EY, Harlos K, Bottomley MJ, Robinson RC, Driscoll PC, Edwards RM, Clements JM, Dudgeon TJ, Stuart DI. Crystal structure of an integrin-binding fragment of VCAM-1 at 1.8 Angstrom resolution. *Nature* 1995; **373**: 539–544.
29. Vonderheide RH, Tedder TF, Springer TA, Staunton DE. Residues within a conserved amino acid motif of domains 1 and 4 of VCAM-1 are required for binding to VLA-4. *J Cell Biol* 1994; **125**: 215–222.
30. Clements JM, Newham P, Shepherd M, Gilbert R, Dudgeon MJ, Needham LA, Edwards RM, Berry L, Brass A, Humphries MJ. Identification of a key integrin-binding sequence in VCAM-1 homologous to the LDV active site in fibronectin. *J Cell Sci* 1994; **107**: 2127–2135.
31. De Fougerolles A, Springer TA. Ideas crystallized on immunoglobulin superfamily-integrin interactions. *Curr Biol* 1995; **2**: 639–643.
32. Cardarelli PM, Cobb RR, Nowlin DM, Scholz W, Gorcsan F, Moscinski M, Yasuhara M, Chiang SL, Lobl TJ. Cyclic RGD peptide inhibits $\alpha 4\beta 1$ interaction with connecting segment 1 and vascular cell adhesion molecule. *J Biol Chem* 1994; **269**: 18668–18673.

33. Wang JH, Pepinsky RB, Stehle T, Liu JH, Karpusas M, Browning B, Osborn N. The crystal structure of an N-terminal two-domain fragment of VCAM-1: a cyclic peptide based on the domain 1 CD-loop can inhibit VCAM-1/α4 integrin interaction. *Proc Natl Acad Sci USA* 1995; **92**: 5714–5718.
34. Rose K. Facile synthesis of homogeneous artificial proteins. *J Am Chem Soc* 1994; **116**: 30.
35. Lu W, Qasim MA, Kent SBH. Comparative total syntheses of turkey ovomucoid third domain by both stepwise solid phase synthesis and native chemical ligation. *J Am Chem Soc* 1996; **118**: 8518–8523.
36. Tuchscherer G. Template assembled synthetic proteins: condensation of a multifunctional peptide to a topological template via chemoselective ligation. *Tetrahedron Lett* 1993; **34**: 8419.
37. Hynes RO. Integrins: versatility, modulation and signaling in cell adhesion. *Cell* 1992; **69**: 11–25.
38. Springer TA. Traffic signals for lymphocyte recirculation and leukocyte emigration: the multistep paradigm. *Cell* 1994; **76**: 301–314.
39. Ruegg C, Postigo AA, Sikorski EE, Butcher EC, Pytela R, Erle DJ. Role of integrin alpha 4 beta 7/alpha 4 beta P inlymphocyte adherence to fibronectin and VCAM-1 and in homotypic cell clustering. *J Cell Biol* 1992; **117**: 179–189.

